The effect of positional isomerism of cyano group of the rod-like mesogens on the liquid crystalline and optical characteristics

Zhigao Liu
China West Normal University
Xiaotong Liu
China West Normal University
Yurun Liang
China West Normal University
Shunbo Zhang
China West Normal University
Xiuning Hu
China West Normal University
Yulong Xiao
ylxiaosc@foxmail.com

China West Normal University

Research Article

Keywords: Liquid crystal, Aggregation-induced emission, Mechanochromism, Cyanostilbene, Pyrene

Posted Date: March 15th, 2024

DOI: https://doi.org/10.21203/rs.3.rs-4089030/v1

Additional Declarations: No competing interests reported.

Abstract

Two novel cyanostilbene-based rod-like mesogens named **BI-CN-4** and **BI-CHO-4** consisting of one terminal pyrene and one terminal alkyl chain were prepared by Suzuki coupling and Knoevenagel reactions. The influence of the positional isomerism of cyano group of cyanostilbene unit on the liquid crystalline characteristics, photophysical characteristics, and mechanochromism characteristics is explored by using POM, DSC, XRD, UV spectra, PL spectra, DFT and TD-DFT calculations. **BI-CN-4** in which the cyano group is adjacent to the phenylpyrene unit exhibits monotropic smectic C phase, whereas **BI-CHO-4** in which the cyano group is far away from the phenylpyrene unit exhibits enantiotropic smectic C phase. **BI-CN-4** exhibits more distinct positive solvatochromism due to more distinct intramolecular charge transfer. Both compounds exhibit AIE or AIEE behavior and reversible mechanochromism behavior due to twisted molecular configurations. These results demonstrated that the distinct molecular design could endow organic molecules with multifunctional properties and potentials.

Introduction

Organic luminescent materials with tunable emission intensity and emitting color in different have obtained much attention and also have been widely applied in various fields including organic light-emitting diodes (OLEDs),[1,2] anti-counterfeiting technology[3,4] and biological imaging[5,6] and others. Among these materials, mechanochromic luminescent materials showed distinct emitting-color changes as a result of the change in molecular packings, intermolecular interactions, morphological structures and molecular conformations induced by mechanical stimuli.[7] In general, the mechanochromic luminescent materials always exhibit strong solid-state emission. However, the conventional organic luminescent materials suffered aggregation-caused quenching (ACQ) due to the strong intermolecular π-π stacking interactions in aggregated state, which hindered the development of mechanochromic luminescent materials. Fortunately, the opposite phenomenon of ACQ called aggregation-induced emission (AIE) or aggregation-induced enhanced emission (AIEE) was discovered by Tang et al. and Park et al. in 1-methyl-1,2,3,4,5-pentaphenylsilole and cyanostilbene molecules.[8,9] Due to the good performance, the AIE- or AIEE- active units are regarded as promising candidates for constructing mechanochromic luminescent materials. Therefore, various mechanochromic luminescent materials containing AIE- or AIEE- active units including cyanostilbene, tetraphenylethylene, dibenzofulvene and *β*-diketonate and others have been developed.[10,11,12,13,14,15,16,17]

Molecular engineering plays an important role in constructing novel photoelectric materials and self-assembly materials. Tuning the chemical structures including the aromatic units, linking groups, appending groups and even the position of lateral/terminal groups of the organic molecules, especially the organic liquid crystalline molecules would induce the great difference of self-assemblies, phase transition temperature, functional properties and others.[18,19,20] For instance, Tschierske and Cheng reported some bolapolyphilic liquid crystals and the changes of the type of rod-like aromatic units and

the length of lateral chains led to various mesophases including lamellar phases, honeycomb columnar phases and different cubic phases.[21,22,23,24] In addition, we also reported some rod-like molecules in which the change of the position of aromatic units led to the transition of mesophases, different AIE behaviors and stimulus-response behaviors.[25,26] Therefore, the exploration of the influence of chemical structures of liquid crystalline molecules on the properties and the understanding of structure-property relationships would be important for the construction of different materials.

Pyrene and cyanostilbene are important functional groups having the good characteristics of high fluorescence quantum efficiency, easy modification and electronic properties to be employed to construct functional materials. Recently, some liquid crystalline materials or/and luminescent materials containing both pyrene and cyanostilbene have been constructed and usually the cyanostilbene was appended to the 1- position, 1,6- positions or/and 1,3,6,8- positions.[26,27,28,29,30] These materials exhibited wonderful self-assembly properties and luminescent properties. Inspired by these good performances, we employed pyrene and cyanostilbene as aromatic units to fabricate two rod-like liquid crystals. And the influence of the positional isomerism of cyano group on the liquid crystalline self-assembly, solvatochromic properties, AIE behaviors and mechanochromic behaviors was investigated. Such investigations have benefits on the understanding of the relationship between chemical structure-properties and also have a great effect on novel multifunctional materials.

Results and Discussion

2.1. Synthesis

The synthesis of the rod-like mesogens mainly involves three key steps including Suzuki coupling reaction, etherification reaction and Knoevenagel condensation reaction as shown in Scheme 1. Firstly, Suzuki coupling reaction pyren-1-ylboronic acid and 4-bromobenzaldehyde or 2-(4-bromophenyl)acetonitrile took place to yield compounds **1**.[31,32] In addition, 4-hydroxybenzaldehyde and 2-(4-hydroxyphenyl)acetonitrile were *o*-alkylated with bromotetradecane in the presence of base to yield compounds **2**. Finally, compounds **1** were reacted with compounds **2** under the Knoevenagel condensation condition to yield the rod-like liquid crystals **BI-CN-4** and **BI-CHO-4**. The synthetic details and corresponding spectrum analysis results were provided in the Supplemental Materials.

2.2. Liquid-crystalline properties

The thermal behavior and optical textures of compounds **BI-CN-4** and **BI-CHO-4** were studied by using polarized optical microscopy (POM) and differential scanning calorimetry (DSC). On heating process of compound **BI-CN-4** under POM, the crystal transformed into the isotropic state at about 175 ℃. On first cooling process from isotropic state of compound **BI-CN-4**, irregular schlieren texture could be observed indicating that compound **BI-CN-4** could self-organize into smectic C phase (Fig. 1a).[33] On heating process of compound **BI-CHO-4** under POM, the crystal gradually transformed into mesophase at about 144 ℃ and then transformed into isotropic state at about 148 ℃, indicating that the mesophase range is

very narrow. On cooling process from isotropic state of compound **BI-CHO-4**, distinct schlieren texture could be observed indicating that compound **BI-CHO-4** could also self-assemble into smectic C phase (Fig. 1b).[16] The phase transition temperatures were further detected by DSC (Fig. 1c and 1d). In the DSC curve of compound **BI-CN-4**, two endothermic peaks at 140.5 ℃ and 170.5 ℃ could be observed in the second heating cycle which corresponded to the phase transition from crystalline state to crystalline state and from smectic C to isotropic state, respectively. Interestingly, there were two exothermic peaks at 89.7 ℃ and 144.8 ℃ which could be attributed to cold-crystallization transition peaks in the second heating cycle. Such exothermic peaks appeared in the second heating cycle might be due to the appearance of metastable structure cooling from isotropic state, which could transform into more stable well-ordered structures *via* endothermal recrystallization process (Fig. 1c). Only one exothermic peak at 131.9 ℃ in the first cooling cycle could be detected which corresponded to the phase transition from isotropic state to smectic C phase (Fig. 1c). In the DSC curve of compound **BI-CHO-4**, four endothermic peaks at 77.3 ℃, 127.8 ℃, 140.5 ℃ and 148.4 ℃ could be observed in the second heating cycle. These peaks at 77.3 ℃ and 127.8 ℃ could be ascribe to the phase transition from crystalline state to crystalline state. The peaks at 140.5 ℃ and 148.4 ℃ could be assigned to the phase transition from crystalline state to smectic C phase and from smectic C phase to isotropic state (Fig. 1d). In the second heating cycle, two exothermic peaks at 139.1 ℃ and 73.1 ℃ could be observed which corresponded to the phase transition from isotropic state to smectic C phase and from smectic C phase to crystalline state, respectively (Fig. 1d). The DSC data were well in line with the observations under POM further demonstrating that compound **BI-CN-4** is monotropic liquid crystal whereas compound **BI-CHO-4** is enantiotropic liquid crystal (Fig. 1a-1d). The difference in thermal behavior and self-assembly behavior of both mesogens could be attributed to the position of cyano group. The cyano group which is adjacent to the phenylpyrene unit could increase the molecular conjugation and finally lead to close molecular stacking. Therefore **BI-CN-4** exhibited much higher melting temperature than that of **BI-CHO-4** and **BI-CHO-4** was more likely to form lamellar structure.

2.3. Solvatochromic properties

The solvatochromic behavior of the pyrene-based liquid crystals was examined in some common organic solvents with different polarities by using absorption and emission spectra (Fig. S1, Fig. 2 and Table S1-2). Both compounds **BI-CN-4** and **BI-CHO-4** display only one absorption band at about 345-359 nm and 362-370 nm, respectively and the absorption bands of **BI-CN-4** and **BI-CHO-4** display little transformation with the change in solvent polarities indicating that the electronic configurations in the ground state are very stable. Both compounds **BI-CN-4** and **BI-CHO-4** also display one emission band at 450 nm and 465 nm in non-polar cyclohexane, respectively. The fluorescence color of compound **BI-CN-4** is relatively weak, in contrast, the fluorescence color of compound **BI-CHO-4** is blue (inset of Fig. 2a-2b). The emission bands of compounds **BI-CN-4** and **BI-CHO-4** gradually red-shift, the fluorescence color of compound **BI-CHO-4** gradually turn yellow-green, but the fluorescence color of compound **BI-CN-4** is hardly detected due to the weak emission in solutions with the increase in solvent polarities (from cyclohexane to dimethyl formamide). These observations indicated that positive solvatochromic behavior could be achieved in **BI-**

CN-4 and **BI-CHO-4**, which might be assigned to the intramolecular charge transfer. The highest occupied molecular orbitals (HOMOs) and the lowest unoccupied molecular orbitals (LUMOs) were obtained by density functional theory (DFT) to visualize the intramolecular charge transfer effect. The HOMOs of compounds **BI-CN-4** and **BI-CHO-4** were primarily situated on the pyrene unit and only a little situated on the cyanostilbene unit. On the contrary, the HUMOs of **BI-CN-4** and **BI-CHO-4** were primarily situated on the cyanostilbene unit and only a little were situated on the pyrene unit. By comparing the emission spectra of both **BI-CN-4** and **BI-CHO-4**, compound **BI-CN-4** exhibited more distinct solvatochromism behavior, which could be assigned to the more distinct charge transfer. The hole-electron examination was employed to explore the differences of charge transfer between **BI-CN-4** and **BI-CHO-4** by using Multiwfn (Fig. 2c).[34] The hole-electron distributions at the excited state demonstrated that the negative charges of **BI-CN-4** and **BI-CHO-4** primarily situated on cyanoethylene and the positive charges of **BI-CN-4** and **BI-CHO-4** primarily situated on pyrene. Therefore, both compounds exhibited distinct charge separation at the excited state. The C_{hole}-C_{ele} diagrams demonstrated that the charge centroids of **BI-CN-4** and **BI-CHO-4** were individual and the D indexes that represented the distance between the centroids of C_{hole} and C_{ele} showed big difference. The D indexes were simulated to be 6.61 Å for $S_0 \rightarrow S_1$ excitation of **BI-CN-4** and 4.09 Å for $S_0 \rightarrow S_1$ excitation of **BI-CHO-4**, respectively (Fig. 2d). The big difference of D indexes indicated that different charge transfer after excitation for both compounds.[35] Therefore, a smaller distance between electron acceptor (cyano group) and electron donor (pyrene) had more greater effect on the charge transfer.

2.4. AIE and AIEE behaviors

Cyanostilbene a typical of AIE and AIEE materials on account of distorted conformation which could restrict intramolecular rotation. In order to explore the AIE and AIEE properties of **BI-CN-4** and **BI-CHO-4**, the absorption and emission spectra in THF-H_2O mixtures with varying proportions of water (f_w: 0%-90%) were studied. The absorption spectra in pure THF exhibited two peaks at 278 nm and 345 nm for **BI-CN-4** and also two peaks at 280 nm and 362 nm for **BI-CHO-4** (Fig. S2). The position and intensity of absorption spectra displayed little change with increasing the f_w from 0% to 90%. The level-off tails of the long-wavelength region emerged when the f_w was higher than 30%, indicating that the aggregates were formed in the mixtures.[36] The emission spectrum of **BI-CN-4** in pure THF exhibited an extremely weak band at 484 nm and the emission spectra displayed little fluctuation when the f_w was lower than 30% (Fig. 3a-b). The position of the emission spectra displayed a little red shift due to the polarity and the intensity showed a little increase due to the formation of aggregates, when the f_w was ranged from 30% to 70%. The emission intensity further increased with increasing the f_w and finally reached to the maximum when the f_w was 90% (Fig. 3a-b). In contrast, the emission spectrum of **BI-CHO-4** in pure THF exhibited a strong band at 493 nm. The position of the emission spectra also showed a little red shift and the intensity showed a little decrease due to the increased polarity of the mixture, when the f_w was ranged from 0% to 60% (Fig. 3c-d). The emission intensity further increased with increasing the f_w and finally reached to the maximum when the f_w was 90% (Fig. 3c-d). These observations in absorption and

emission spectra in THF-H_2O mixtures of **BI-CN-4** and **BI-CHO-4** demonstrated that **BI-CN-4** and **BI-CHO-4** exhibited AIE and AIEE behaviors, respectively.

2.4. Mechanochromic behaviors

The mechanochromic behaviors of **BI-CN-4** and **BI-CHO-4** in of the pristine, ground, and fumed states were also explored by the absorption and emission spectra, fluorescence lifetimes, powder X-ray diffraction analysis and differential scanning calorimetry curves. Both compounds **BI-CN-4** and **BI-CHO-4** display a blue-emission band at 472 nm and 474 nm in the pristine state, respectively (Fig. S3 and Fig. 4). The fluorescence lifetimes of **BI-CN-4** and **BI-CHO-4** were about 1.89 ns and 2.40 ns, respectively (Fig. 4e-f). After **BI-CN-4** was ground in mortar for several minutes, the emission spectrum showed obvious red shift to 498 nm, the fluorescent color turned into blue-green and the fluorescence lifetimes showed little fluctuation to 1.87 ns (Fig. 4a, 4c and 4e). For **BI-CHO-4**, the emission spectrum showed more obvious red shift to 512 nm, the fluorescent color turned yellow-green and the fluorescence lifetimes showed obvious increase to 4.26 ns (Fig. 4b, 4d and 4f) after grinding in mortar for several minutes. After fuming with *n*-hexane for several minutes, the emission spectra of **BI-CN-4** and **BI-CHO-4** recovered to the original state. The reversible changes could be attributed to the change of molecular stacking and molecular conformation caused by the external mechanical force and further solvent fuming.

In order to explain the mechanism of mechanochromic behavior of **BI-CN-4** and **BI-CHO-4**, powder X-ray diffraction and differential scanning calorimetry investigations were conducted. The powder X-ray diffraction patterns of **BI-CN-4** and **BI-CHO-4** in the pristine state clearly showed several intensive and sharp reflection peaks at 5°-40° indicating well-ordered molecular stacking (Fig. 5a-b). After **BI-CN-4** and **BI-CHO-4** were ground in mortar for several minutes, some characteristic peaks became weak and even disappeared demonstrating that the molecular stacking became disordered. Further, after fuming with *n*-hexane for several minutes, the peaks appeared again demonstrating that the well-ordered molecular stacking recovered by fuming (Fig. 5a-b). Additionally, the DSC curves of the pristine solid of **BI-CN-4** and **BI-CHO-4** for the first heating cycle only showed one endothermic peak at 173.4 ℃ and 150.7 ℃, respectively, which could be attributed the phase transition from solid state to liquid state (Fig. 5c-d). After **BI-CN-4** and **BI-CHO-4** were ground in mortar for several minutes, the DSC curves of the ground solid of **BI-CN-4** and **BI-CHO-4** for the first heating cycle appeared one new exothermic peak at 53.6 ℃ and 54.1 ℃, respectively, which could be attibuted to thermal crystallization peak, demonstrating that the amorphous state could be formed by grinding (Fig. 5c-d). Therefore, the change in molecular stacking and formation of amorphous state by grinding would be responsible for the mechanochromic behaviors.

Conclusion

In summary, two novel rod-like liquid crystalline molecules with distinct self-assembly, solvatochromic properties, AIE behaviors and mechanochromic behaviors were designed. The positional isomerism of cyano group induced the transition of from the monotropic smectic C phase to enantiotropic smectic C phase. The cyano group which was adjacent to pyrene induced more distinct solvatochromic behaviors

due to the charge transfer. The distorted molecular conformation endowed the rod-like liquid crystalline molecules AIE or AIEE behaviors. The mechanochromic luminescence investigation demonstrated that both liquid crystalline molecules exhibited reversible mechanochromism natures with high contrast change in fluorescent color due to the change in molecular stacking and the state of solid. These investigations give a new strategy for the design and synthesis of multifunctional materials.

Declarations

Conflict of interest: There are no conflicts of interest to declare.

Consent to Participate: All authors approved their consent in the participation of their work in the manuscript.

Consent for Publication: All authors read the manuscript and given their consent to publish the work.

Data Availability: All data generated and analyzed during the current study are included in the article and Supplementary Materials file.

Ethical Approval: This article does not contain any studies with human or animal subjects.

Authorship contribution

Zhigao Liu: Data curation; Investigation.

Xiaotong Liu: Investigation; Writing-original draft; Writing-review & editing.

Yurun Liang: Investigation.

Shunbo Zhang: Investigation.

Xiuning Hu: Investigation.

Yulong Xiao: Conceptualization; Funding acquisition; Methodology; Project administration; Resources; Writing-original draft; Writing-review & editing.

Funding

This work was supported by China West Normal University Doctor Startup Fund (No. 412821), Major project funds of Chemical Synthesis and Pollution Control Key Laboratory of Sichuan Province (No. CSPC202101), The Science and Technology Department of Sichuan Province (No. 2022NSFSC1237) and Innovation and entrepreneurship training program for college students (No. S202310638056).

References

1. S. Tan, K. Jinnai, R. Kabe, C. Adachi. Long-persistent luminescence from an exciplet-based organic light-emitting diodes, Adv. Mater. 33 2008844 (2021). https://doi.org/10.1002/adma.202008844
2. R. De, S.K. Pal, Self-assembled discotics as molecular semiconductors, Chem. Commun. 59 3050-3066 (2023). https://doi.org/10.1039/D2CC06763C
3. M.Q. Li, Q. Zhang, J.R. Wang, X.F. Mei, Mechanochromism triggered fluorescent color switching among polymorphs of a natural fluorescence pigment, Chem. Commun. 52 11288-11291 (2016). https://doi.org/10.1039/C6CC04958C
4. G. Huang, Q. Xia, W. Huang, J. Tian, Z. He, B.S. Li, B.Z. Tang, Multiple anti-counterfeiting guarantees from a simple tetraphenylethylene derivative-high-contrasted and multi-state mechanochromism and photochromism, Angew. Chem. Int. Ed. 58 17814-17819 (2019). https://doi.org/10.1002/anie.201910530
5. Z. Yang, Z. Mao, Z. Xie, Y. Zhang, S. Liu, J. Zhao, J. Xu, Z. Chi, Aldred MP. Recent advances in organic thermally activated delayed fluorescence materials. Chem. Soc. Rev. 46 915-1016 (2017). https://doi.org/10.1039/C6CS00368K
6. X. Tian, L.C. Murfin, L. Wu, S.E. Lewis, T.D. James, Fluorescent small organic probes for biosensing. Chem. Sci. 12 3406-3426 (2017). https://doi.org/10.1039/D0SC06928K
7. Z. Chen, D.D. Deng, S.Z. Pu, Recent advances in aggregation-induced emission (AIE)-active tetraphenylethylene-modified luminophores with mechanochromic luminescence characteristics, Tetrahedron Lett. 107 154096 (2022). https://doi.org/10.1016/j.tetlet.2022.154096
8. J.D. Luo, Z. Xie, J.W.Y. Lam, L. Cheng, H.Y. Chen, C.F. Qiu, H.S. Kwok, X.W. Zhan, Y.Q. Liu, D.B. Zhu, B.Z. Tang, Aggregation-induced emission of 1-methyl-1,2,3,4,5-pentaphenylsilole. Chem Commun. 18 1740-1741 (2001). https://doi.org/10.1039/B105159H
9. B.K. An, S.K. Kwon, S.D. Jung, S.Y. Park, Enhanced emission and its switching in fluorescent organic nanoparticles, J. Am. Chem. Soc. 124 14410-14415 (2002). https://doi.org/10.1021/ja0269082
10. S.J. Yoon, S.Y. Park, Polymorphic and mechanochromic luminescence modulation in the highly emissive dicyanodistyrylbenzene crystal: secondary bonding interaction in molecular stacking assembly. J. Mater. Chem. 21 8338-8346 (2011). https://doi.org/10.1039/C0JM03711G
11. J. Zhao, Z. Chi, Y. Zhang, Z. Mao, Z. Yang, E. Ubba, Z.G. Chi, Recent progress in the mechanofluorochromism of cyanoethylene derivatives with aggregation-induced emission. J. Mater. Chem. C. 6 6327-6353 (2018). https://doi.org/10.1039/C8TC01648H
12. X. Luo, J. Li, C. Li, L. Heng, Y.Q. Dong, Z. Liu, Z.S. Bo, B.Z. Tang, Reversible switching of the emission of diphenyldibenzofulvenes by thermal and mechanical stimuli, Adv. Mater. 23 3261-3265 (2011). https://doi.org/10.1002/adma.201101059
13. Z. Zhao, T. Chen, S. Jiang, Z. Liu, D. Fang, Y.Q. Dong, The construction of a multicolored mechanochromic luminogen with high contrast through the combination of a large conjugation core and peripheral phenyl rings, J. Mater. Chem. C. 4 4800-4804 (2016). https://doi.org/10.1039/C6TC00972G

14. S. Gundu, M. Kim, N. Mergu, Y.A. So, AIE-active and reversible mechanochromic tetraphenylethene-tetradiphenylacrylonitrile hybrid luminogens with re-writable optical data storage application, Dyes Pigm. 146 7-13 (2017). http://dx.doi.org/10.1016/j.dyepig.2017.06.043
15. T. Butler, W.A. Morris, J.S. Kosicka, C.L. Fraser, Mechanochromic luminescence and aggregation induced emission of dinaphthoylmethane β-diketones and their boronated counterparts, ACS Appl. Mater. Interfaces. 8 1242-1251 (2016). https://doi.org/10.1021/acsami.5b09688
16. Z. Yang, Z. Chi, Z. Mao, Y. Zhang, S. Liu, J. Zhao, M.P. Aldred, Z.G. Chi, Recent advances in mechano-responsive luminescence of tetraphenylethylene derivatives with aggregation-induced emission properties, Mater. Chem. Front. 2 861-890 (2018). https://doi.org/10.1039/C8QM00062J
17. Q. Qi, J. Qian, X. Tan, J. Zhang, L. Wang, B. Xu, B. Zou, W.J. Tian, Remarkable turn-on and color-tuned piezochromic luminescence: mechanically switching intramolecular charge transfer in molecular crystals, Adv. Funct. Mater. 25 4005-4010 (2015). https://doi.org/10.1002/adfm.201501224
18. T. Wöhrle, I. Wurzbach, J. Kirres, A. Kostidou, N. Kapernaum, J. Litterscheidt, J.C. Haenle, P. Staffeld, A. Baro, F. Giesselmann, S. Laschat, Discotic liquid crystals, Chem. Rev. 116 1139-1241 (2016). https://doi.org/10.1021/acs.chemrev.5b00190
19. C. Tschierske, Development of structural complexity by liquid-crystal self-assembly, Angew. Chem. Int. Ed. 52 8828-8878 (2013). https://doi.org/10.1002/anie.201300872
20. K. Goossens, K. Lava, C.W. Bielawski, K. Binnemans, Ionic liquid crystals: Versatile materials, Chem. Rev. 116 4643-4807 (2016). https://doi.org/10.1021/cr400334b
21. X.H. Cheng, H.F. Gao, X.P. Tan, X.Y. Yang, M. Prehm, H. Ebert, C. Tschierske, Transition between triangular and square tiling patterns in liquid-crystalline honeycombs formed by tetrathiophene-based bolaamphiphiles, Chem. Sci. 4 3317-3331 (2013). https://doi.org/10.1039/C3SC50664A
22. C.L. Chen, R.t Kieffer, H. Ebert, M. Prehm, R.B. Zhang, X.B. Zeng, F. Liu, G. Ungar, C. Tschierske, Chirality induction through nano-phase separation: Alternating network gyroid phase by thermotropic self-assembly of X-shaped bolapolyphiles, Angew. Chem. Int. Ed. 59 2725-2729 (2020). https://doi.org/10.1002/anie.201911245
23. S. Poppe, M. Poppe, H. Ebert, M. Prehm, C. Chen, F. Liu, S. Werner, K. Bacia, C. Tschierske, Effects of lateral and terminal chains of X-shaped bolapolyphiles with oligo(phenylene ethynylene) cores on self-assembly behaviour. Part 1: Transition between amphiphilic and polyphilic self-assembly in the bulk. Polymers. 9 471 (2017). https://doi.org/10.3390/polym9100471
24. C.L. Chen, M. Poppe, S. Poppe, M. Wagner, C. Tschierske, F. Liu, Tetrahedral liquid-crystalline networks: An A15-like frank-kasper phase based on rod-packing, Angew. Chem. Int. Ed. 61 202203447 (2022). https://doi.org/10.1002/anie.202203447
25. N.N. Li, Y.R. Liang, X.T. Liu, G.M. Liang, Q.Y. Zhang, R.L. Zhang, H.F. Gao, Y.L. Xiao, Positional isomerism mediated the self-assembly and optical properties of amphiphilic cyanostyrene-based mesogens, J. Lumin. 258 119810 (2023). https://doi.org/10.1016/j.jlumin.2023.119810
26. M.S. Zeng, Y.R. Liang, N.N. Liu, X.T. Liu, Y.L. Xiao, Impact of the position of nitrogen atom on the liquid crystal, optical and multi-stimuli response behaviors of rod-like mesogens containing multiple

functional building blocks, J. Lumin. 267 120375 (2024). https://doi.org/10.1016/j.jlumin.2023.120375

27. Y.Q. Chen, Y.C. Li, Y.R. Liang, X.T. Liu, Y.L. Xiao, The effect of the number of cyanostilbene building blocks on the self-assembly and photophysical property of pyrene-based liquid crystals, Tetrahedron, 149 133742 (2023). https://doi.org/10.1016/j.tet.2023.133742
28. Z. Huang, F. Tang, F. He, L. Kong, J.Y. Huang, J.X. Yang, A.X. Ding, Pyrene and triphenylamine substituted cyanostyrene and cyanostilbene derivatives with dual-state emission for high-contrast mechanofluorochromism and cell imaging, Org. Chem. Front. 9 5118-5124 (2022). https://doi.org/10.1039/D2QO01192A
29. W.Y. Zhao, Z.Y. Ding, Z.Q. Yang, T. Lu, B. Yang, S.M. Jiang, Remarkable off–on tunable solid-state luminescence by the regulation of pyrene dimer, Chem. Eur. J. 30 2023032 (2024). https://doi.org/10.1002/chem.202303202
30. X.H. Wang, L.R. Wang, X.Y. Mao, Q.S. Wang, Z.F. Mu, L. An, W. Zhang,c X. Feng, C. Redshaw, C.Y. Cao, A.J. Qin, B.Z. Tang, Pyrene-based aggregation-induced emission luminogens (AIEgens) with less colour migration for anti-counterfeiting applications, J. Mater. Chem. C. 9 12828-12838 (2021). https://doi.org/10.1039/D1TC03022A
31. J. Qu, Q. Zhang, X.M. Liao, C.Y. Song, X. Meng, Y.C. He, Z. Li, X.X. Zhang, Z.P. Cao, Chiral dual core chromophores based on binaphthyl acrylonitrile motif with tunable dual emission bands and anti-counterfeiting, Chem. Eur. J. 29 202301766 (2023). https://doi.org/10.1002/chem.202301766
32. A. Kathiravan, V. Srinivasan, T. Khamrang, M. Velusamy, M. Jaccob, N. Pavithra, S. Anandan, K. Velappan, Pyrene based D-π-A architectures: synthesis, density functional theory, photophysics and electron transfer dynamics, Phys. Chem. Chem. Phys. 19 3125-3135 (2017). https://doi.org/10.1039/C6CP08180K
33. I. Dierking, Textures of liquid crystals, (Wiley-VCH, Weinheim, 2003), pp. 91-122.
34. T. Lu, F. Chen, Multiwfn: A multifunctional wavefunction analyzer, J. Comput. Chem. 33 580-592 (2012). https://doi.org/10.1002/jcc.22885
35. Y.N. Han, T. Zhang, X.Y. Chen, Q. Chen, P.C. Xue, Spacer group-controlled luminescence and response of C3-symmetric triphenylamine derivatives towards force stimuli, CrystEngComm. 23 202-209 (2021). https://doi.org/10.1039/D0CE01539C
36. J. Liang, Z. Chen, L. Xu L, J. Wang, J. Yin, G.A. Yu, Z. N. Chen, S.H. Liu, Aggregation-induced emission-active gold(i) complexes with multi-stimuli luminescence switching, J. Mater. Chem. C. 2 2243-2250 (2021). https://doi.org/10.1039/C3TC31638F

Scheme 1

Scheme 1 is available in the Supplementary Files section.

Figures

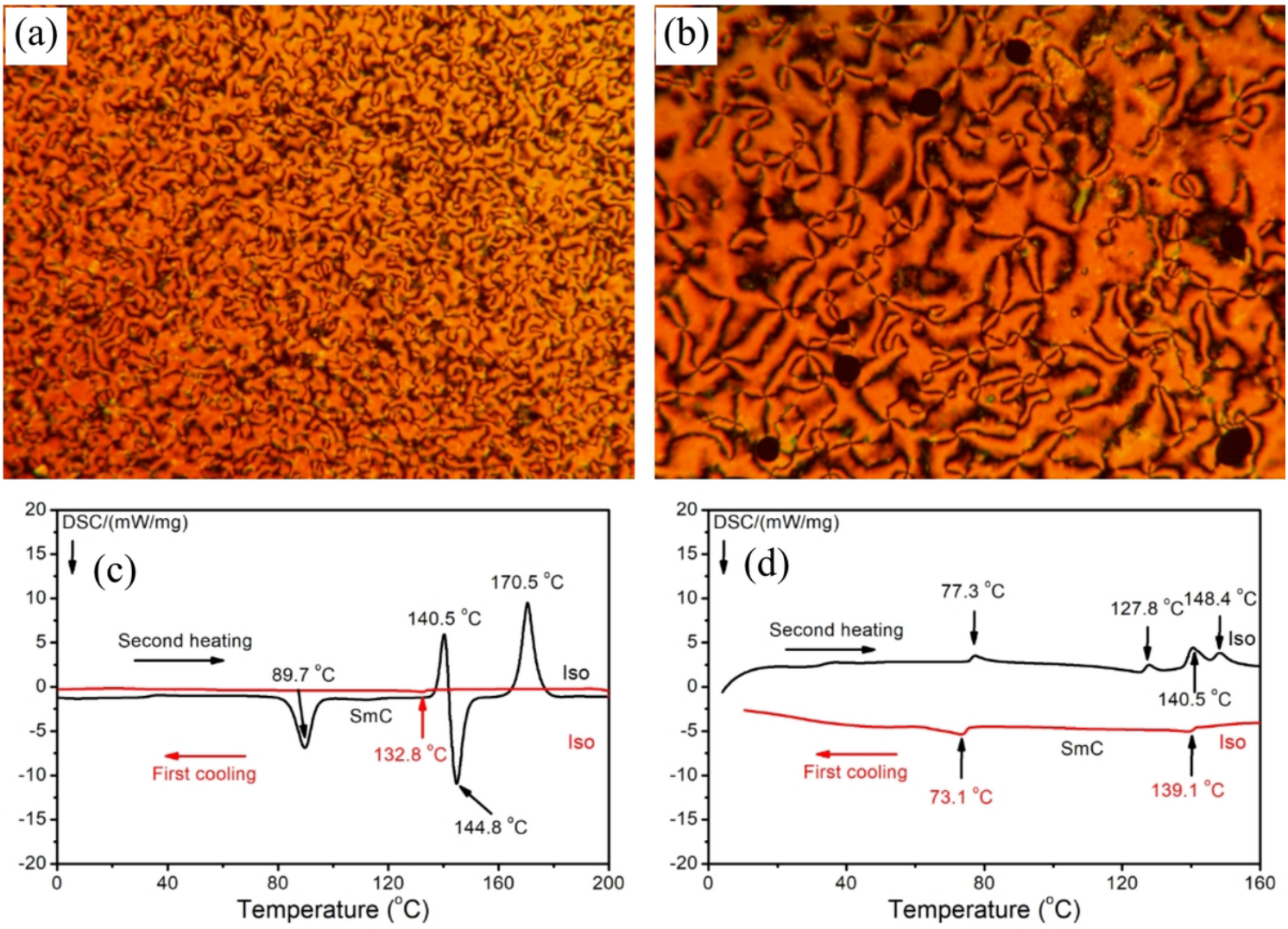

Figure 1

POM textures of (a) **BI-CN-4** cooling at 120 ℃ and (b) **BI-CHO-4** cooling at 100 ℃; DSC thermograms of (c) **BI-CN-4** and (d) **BI-CHO-4** in the first cooling and second heating cycles.

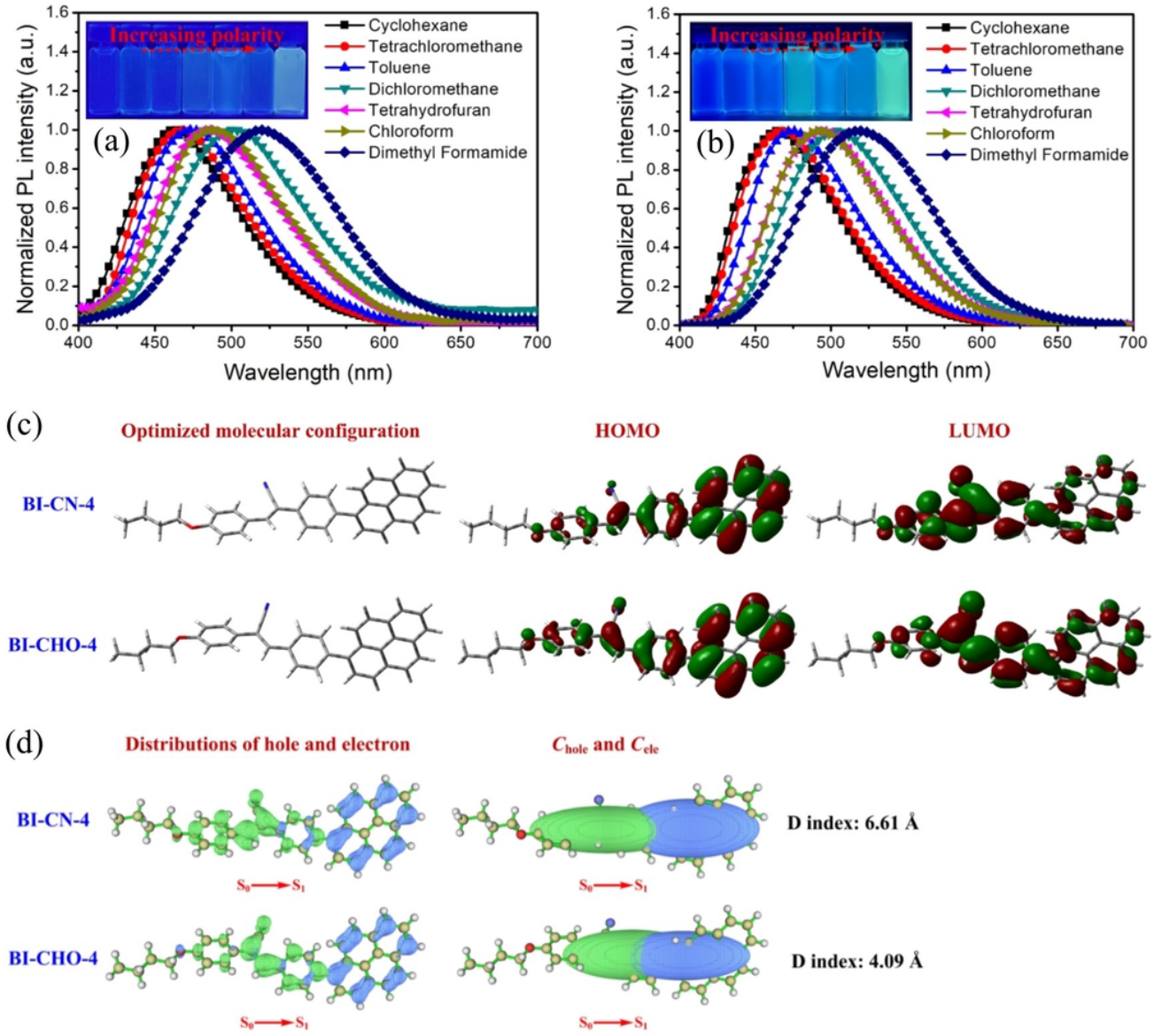

Figure 2

Emission spectra of (a) **BI-CN-4** and (b) **BI-CHO-4** in different solvents, the insets of (a) and (b) show the corresponding fluorescence images; (c) the optimized molecular configuration, HOMO and LUMO of **BI-CN-4** and **BI-CHO-4**; (d) distributions of hole and electron, and C_{hole} and C_{ele} of **BI-CN-4** and **BI-CHO-4**.

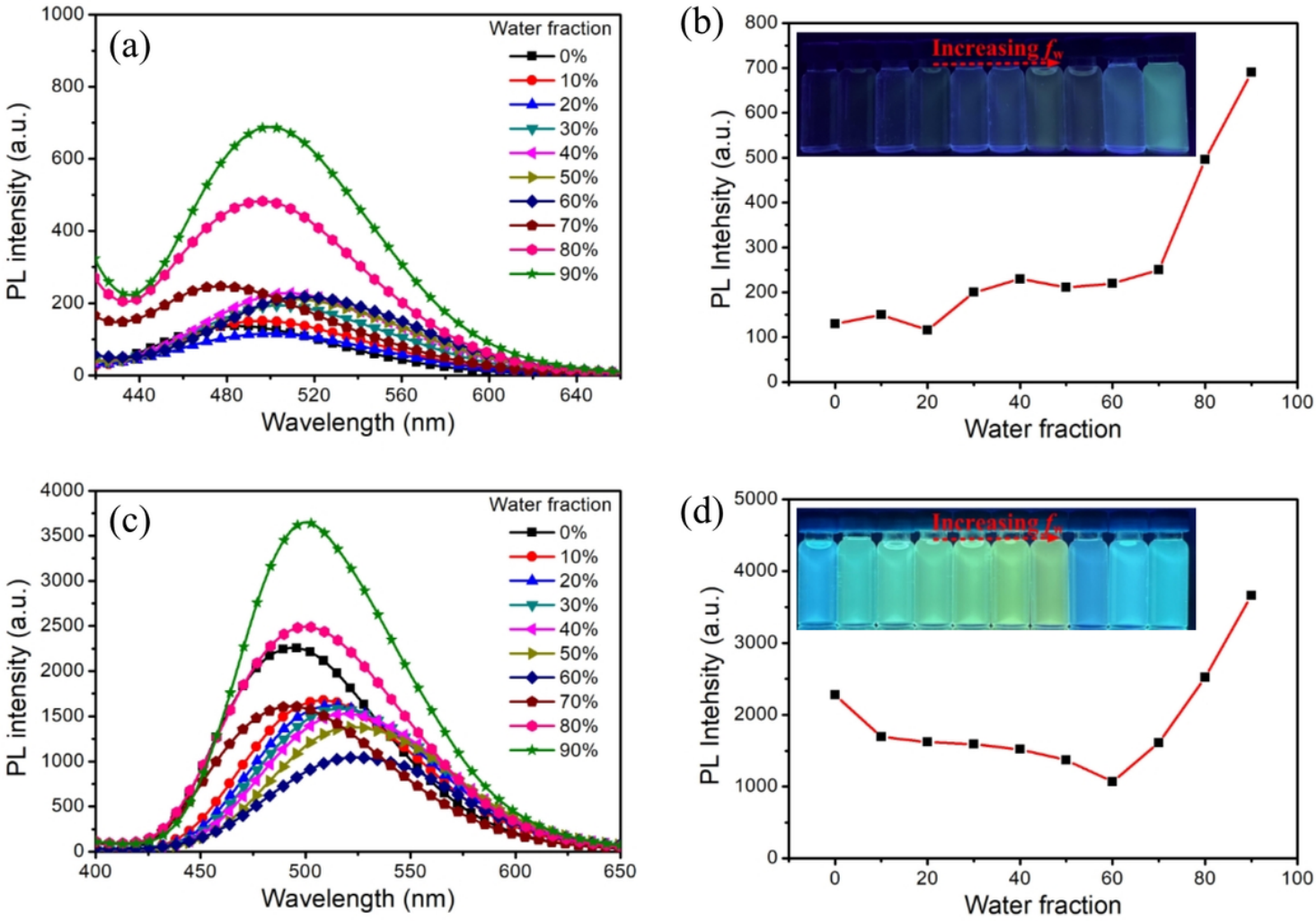

Figure 3

Emission spectra of (a) **BI-CN-4** and (c) **BI-CHO-4** in the mixture of water and tetrahydrofuran with alterative f_w; (b) and (d) plot of relative emission peak intensity *vs* f_w, the insets of (b) and (d) show the corresponding fluorescence images.

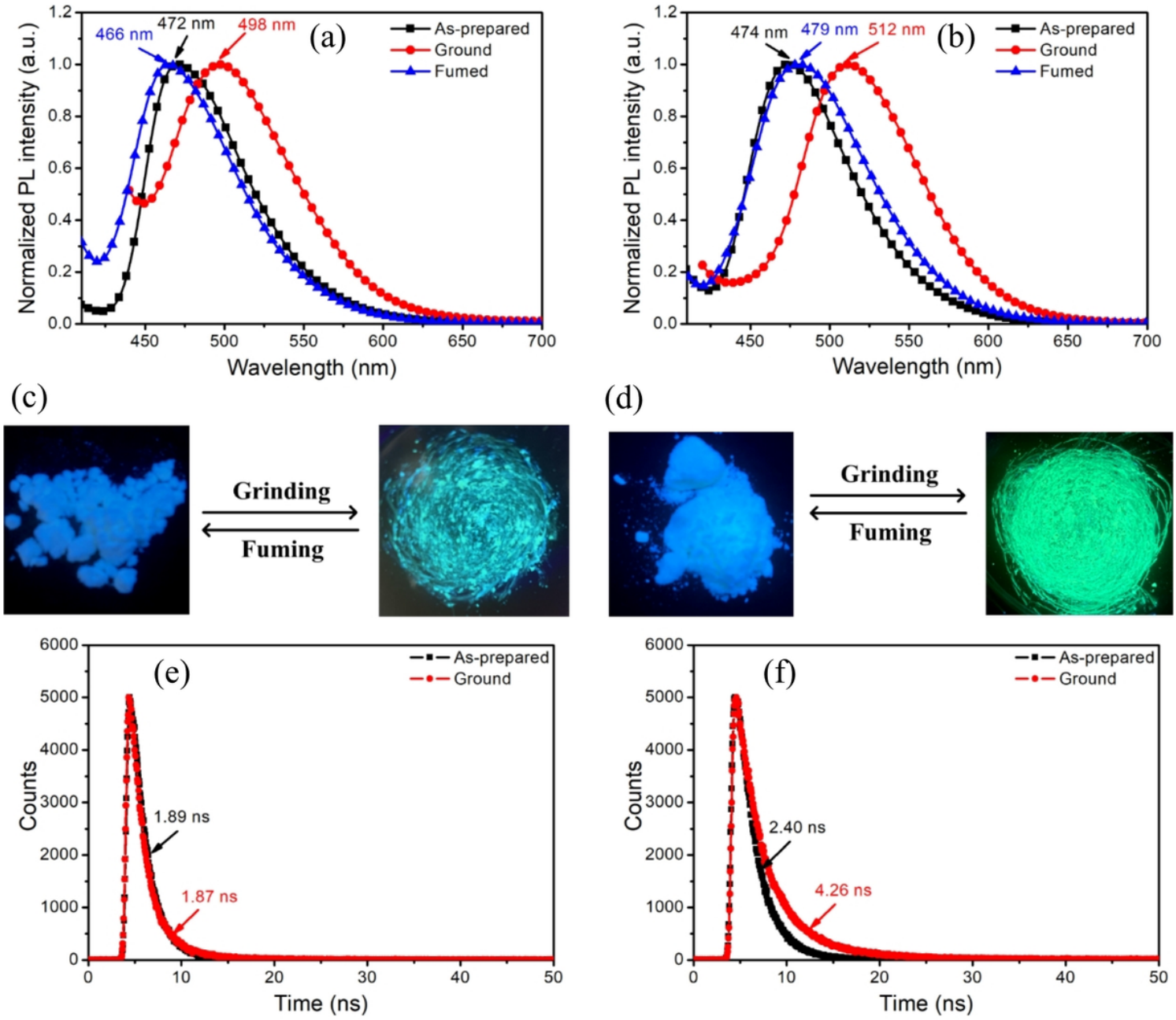

Figure 4

Normalized emission spectra of (a) **BI-CN-4** and (b) **BI-CHO-4**in solid states (as-prepared, ground and fumed); the fluorescence images of (c) **BI-CN-4** and (d) **BI-CHO-4**in solid states before being ground and fumed; Fluorescence decay profiles of(e) **BI-CN-4** and (f) **BI-CHO-4** solid states before/after being ground.

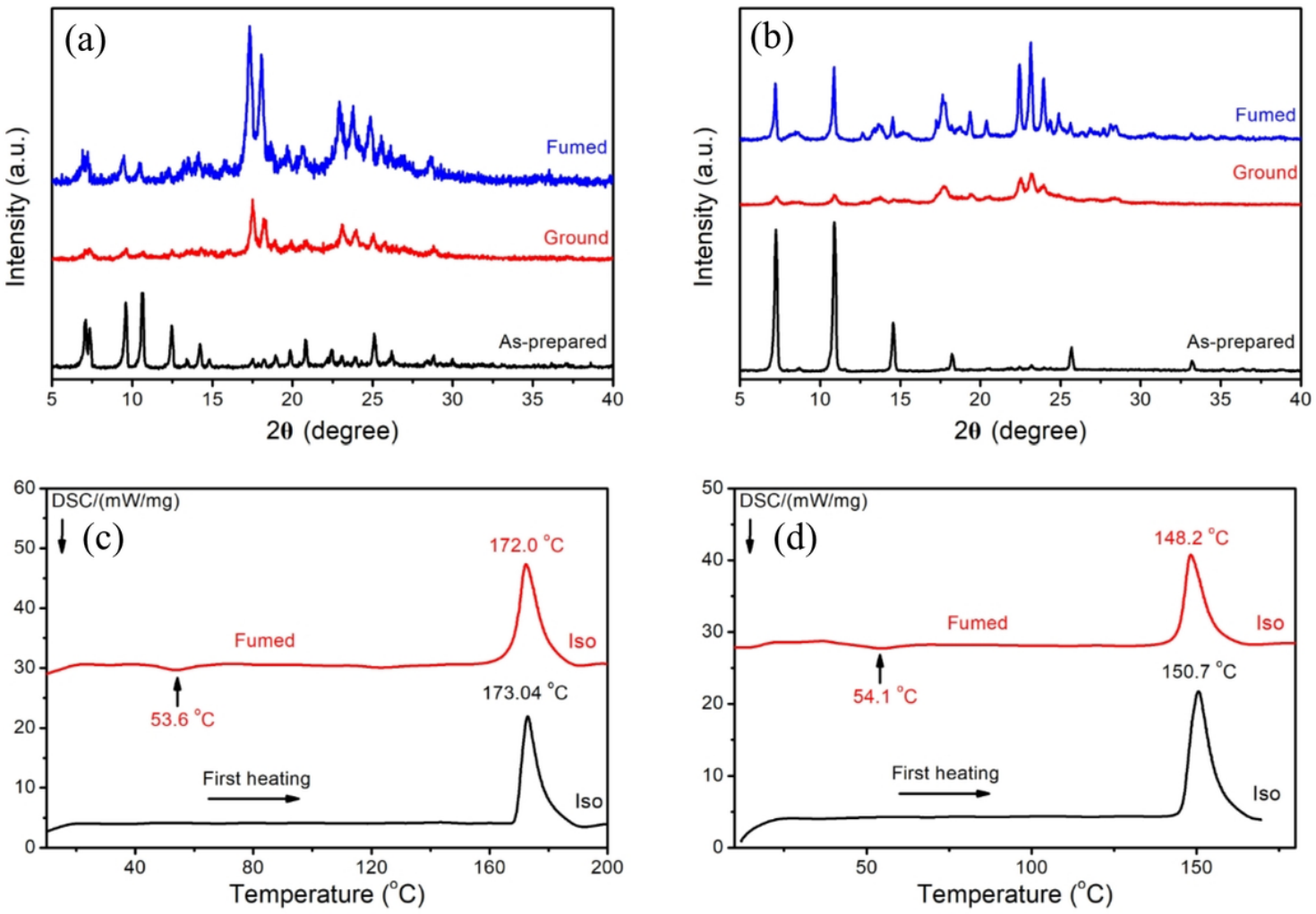

Figure 5

powder X-ray diffractions of (a) **BI-CN-4** and (b) **BI-CHO-4**in solid states (as-prepared, ground and fumed); DSC curves of(c) **BI-CN-4** and (d) **BI-CHO-4** solid states before/after being ground.

Supplementary Files

This is a list of supplementary files associated with this preprint. Click to download.

- SupplementaryMaterials.doc
- Scheme1.png